



HAL
open science

Three-level coordination in power system stabilization

Bogdan Marinescu, David Petesch

► **To cite this version:**

Bogdan Marinescu, David Petesch. Three-level coordination in power system stabilization. *Electric Power Systems Research*, 2014, 111, pp.40 - 51. 10.1016/j.epsr.2014.01.019 . hal-01421773

HAL Id: hal-01421773

<https://hal.science/hal-01421773v1>

Submitted on 9 Jan 2017

HAL is a multi-disciplinary open access archive for the deposit and dissemination of scientific research documents, whether they are published or not. The documents may come from teaching and research institutions in France or abroad, or from public or private research centers.

L'archive ouverte pluridisciplinaire **HAL**, est destinée au dépôt et à la diffusion de documents scientifiques de niveau recherche, publiés ou non, émanant des établissements d'enseignement et de recherche français ou étrangers, des laboratoires publics ou privés.

Three-Level Coordination in Power System Stabilization

Bogdan Marinescu and David Petesch

B. Marinescu is with Département Expertise Système, Réseau de Transport d'Electricité, 9, rue de la Porte de Buc, 78000 Versailles, France, phone 33-1-39 24 40 17, fax 33-1-39 24 41 75, Email: bogdan.marinescu@rte-france.com and also with SATIE-Ecole Normale Supérieure de Cachan
D. Petesch is with Centre National d'Expertise Réseau, Réseau de Transport d'Electricité, Coeur Défense - 100, Esplanade du Général de Gaulle - Tour B, 92932 Paris La Défense Cedex, phone 33-1-79 24 85 48, Email: david.petesch@rte-france.com

Abstract

This paper presents a new methodology for the synthesis of Power System Stabilizers (PSSs) and speed governors in order to satisfy some recent objectives and constraints imposed by the evolution of large-scale interconnected power systems. As a consequence of the increasing size of these systems, the frequency of some inter-area modes diminish so much so that these oscillatory phenomena interact with the dynamics of the speed governors. These low-frequency inter-area modes are also more spread (i.e., they involve a larger number of generators) than the other inter-area modes of the system. These two particularities require several supplementary levels of coordination when tuning the PSSs and the governors of the machines involved in these oscillatory phenomena. To ensure this, the synthesis of the aforementioned regulators is done using a new control model which takes into account the key interactions of the dynamics of the power system. It thus allows the coordination of control actions among several generators as well as between the electrical and mechanical paths. This control framework ensures also an optimal trade-off performance/robustness. Validation simulations have been carried out with the Eurostag software on a realistic large-scale model of the interconnected European power system.

Keywords: PSS tuning, robustness, coordination, speed governors.

1. Introduction

Power system stability analysis is generally done in a local way, i.e., study of the local oscillatory phenomena or the so-called *local modes* which frequency is usually around 1Hz. The power system stabilizers (PSS), which are additional voltage regulation loops for the generators, are used to damp these local modes. In power systems there are also *global* oscillatory phenomena, i.e., the so-called *inter-area* modes (see, e.g., [1]). For the European system, the frequencies of these modes actually range between 0.4 and 0.17Hz. The inter-area modes have also to be damped using the same PSS loops used for the local modes which must thus be tuned (at least) for these two objectives. Notice that the frequency ranges of the two phenomena are slightly different. This is called in the sequel the *first level of coordination*.

Contrary to the local modes, the inter-area modes present two properties. First, they involve a large number of distant machines. Indeed, the damping cannot be achieved by tuning only one PSS, coordination between the tuning actions for different machines must also be envisaged. This is a *second level of coordination* which is required.

To ensure the two above mentioned levels of coordination, information from the whole system should be taken into account when tuning the parameters of the PSS. One way to do this is to use distant measures which can be provided by wide-area measurement systems (WAMS). An alternative is to use a reduced-order model of the whole system, called a *control model*. This second path is followed here as it does not need extra material for the implementation. In [2] and related references, the control model is obtained by reducing a time-domain model of the overall power system using standard balancing techniques. Other approaches use diagonal modal decomposition for the same scope. None of these approaches can be used for large-scale systems. To overcome this difficulty, we developed here a reduced-order model directly focused on the modes of interest, i.e., the modes to be damped. This model is refined by frequency identification for which only a frequency response (Bode plots) is necessary. The latter can be easily obtained even for large-scale models as indicated in Section 2. This kind of control model is of very low order and can be considered as an extension of the one usually used for the tuning of PSS and which consists of the sensitivities of the modes of interest with respect to the gains of the PSSs (see, e.g., [3]). It can be alternatively obtained by time-domain identification as in [4], [5], [6] and related references.

Next, the frequency of the inter-area modes depend on the size of the power system. The connection of the Turkey zone to the ENTSO-E (European Network of Trans-

mission System Operators for Electricity) synchronous zone led to a new inter-area mode at 0.17Hz. Notice that before this extension, the slowest European inter-area mode was at 0.22Hz. Moreover, the latest ENTSO-E interconnection feasibility study [7] has shown that, with this latter potential extension, an inter-area mode at 0.07Hz may exist. Low frequency inter-area modes have already been identified on the Hydro-Québec network [4] and across the interconnection between the Northwest and Southwest American power systems [8]. When the frequencies of the inter-area modes diminish so much, these oscillatory phenomena interact with the dynamics of the speed governors as shown in [1]. These interactions have been taken into account in the work presented here by coordinating the synthesis of the PSSs with the one of the speed governors. This corresponds to a *third level of coordination*. It has already been shown in [8] that the governors can be used to damp system oscillations. In [9] these oscillations are "filtered" at the governor loop level. In [10], modern control methods are used to re-design at a glance the AVR and the governor functions of a given system which leads to a new controller given in a general (i.e., state-space) form. In the present work, standard PSSs (i.e., generally IEEE lead-lag forms [11] used in practice) are tuned in a coordinated manner with supplementary control actions in standard governors. For this, the control model mentioned above is extended in order to take into account the governor's dynamics.

Robustness is an important topic in modern control, especially in the case of power systems where, due to the large scale of the problem, the models used for the dynamic studies are a priori simplified. A lot of work has been dedicated to robust control techniques. The more direct approach consists in tuning the parameters of given standard PSSs' structures in order to achieve the desired performances and level of robustness. This leads to a problem of optimization under constraints [12], [13]. This framework has been used in the work reported here for the tuning of fixed standard structures of PSSs and speed governors for several machines in order to ensure the multilevel coordinations specified above.

The paper is organized as follows: in Section 2, a control model is built for the first two levels of coordination. It is further used in Section 3 for the control synthesis. In Section 4 it is explained why and how the synthesis of the PSSs and governors should be coordinated. The control model introduced in Section 2 as well as the control method in Section 3 are extended in Section 5 to the general case in which all the three levels of coordination can be achieved. Section 6 is devoted to conclusions and remarks.

All the simulations presented in this paper are carried out with the Eurostag transient stability simulator software [14].

2. Multi-frequency control model

2.1. Degrees of detail of the modeling

To synthesize a regulator, a reduced order dynamic model is needed for the system to be controlled. It is called *a control model* and its particularity is to capture only the features which are relevant to the control objectives. In general, the control model most used for the machines of the power systems consists in a machine connected to an infinite bus through a line of variable reactance. The value of the reactance of this line is used to model the short-circuit power at the grid bus to which the machine is connected. However, doing so, it is difficult to capture both local and inter-area oscillatory phenomena especially when they are of quite different frequencies. To move towards a coordination of tuning of the PSSs for several local and inter-area modes in the new context mentioned in the Introduction, *sensitivities* between the damping of the modes of interest and the gains of the PSSs selected for tuning were used as a control model in [3] and related references as follows : the sensitivity of a closed-loop eigenvalue λ_i with respect to the gain K_j of the PSS transfer function $\Gamma_j(s)$ is given by [15]

$$\frac{\partial \lambda_i}{\partial K_j} = r_i^{jj} \quad (1)$$

where r_i^{jj} is the residue of λ_i in the open-loop transfer function $H_{jj}(s)$ from V_{s_j} to ω_j in Fig. 1. V_{s_j} is the stabilizing signal of the AVR of machine j , while ω_j is the speed of the same machine. Notice also that the transfer function mentioned above is computed *before* the installation of the PSS $\Gamma_j(s)$.

This residue can be computed from the right (v_i) and the left (w_i) eigenvectors of λ_i and the input (B_j), respectively the output (C_j) matrices of a minimal state-space realization of $H_{jj}(s)$:

$$r_i^{jj} = C_j v_i w_i^T B_j. \quad (2)$$

The residues in (2) are usual outputs of softwares for small-signal analysis like, *e.g.*, [16]. From (1) one deduces the impact of small variations of the gain K_j of the modes of interest:

$$\lambda_i = \lambda_i^0 + r_i K_j \quad (3)$$

where λ_i^0 is the mode computed on the open-loop, *i.e.*, the situation in Fig. 1 without $\Gamma_j(s)$.

However, this static characterization can be further enriched to take into account the dynamics of interest of the overall system. Overall dynamic models are usually available for the interconnected systems. They consist in a detailed model of the machines of the system of significant installed power (usually the ones of more than 100 MW) along with their regulations and the 400 kV/220 kV transmission grid (see [17] and [7] for the case of the European system). Although simplified with respect to reality, this kind of model, called *simulation model* is too complex (about 20000 state variables in the case of the European system) for a control model. It is used for the full nonlinear simulation of the behavior of the power system, in particular for *a posteriori* validation of an *already synthesized* controller. However, it can be used to extract a suitable control model as shown below.

2.2. Choice of the control model structure

Let $\Lambda = \{\lambda_1, \dots, \lambda_l\}$ be the oscillatory modes (local and inter-area) to be damped and $M = \{M_1, \dots, M_m\}$ the machines for which PSS loops have been chosen to be installed or adapted to perform the damping task. The latter are among the machines with the greatest participation factors in the modes in the set Λ . The way to choose these machines have been addressed in several preceding works (see, e.g., [1], [3]) and the set M is considered here as input data.

The control model concerns the power system seen from the PSSs (see Fig. 1), *i.e.*, the transfer matrix $H(s)$ between the stabilizing signals V_{s_i} of the PSS loops of the machines in the set M and their speeds ω_j :

$$\omega(s) = H(s)V_s(s) \quad (4)$$

where

$$\omega(s) = \begin{bmatrix} \omega_1(s) \\ \vdots \\ \omega_m(s) \end{bmatrix} \text{ and } V_s(s) = \begin{bmatrix} V_{s_1}(s) \\ \vdots \\ V_{s_m}(s) \end{bmatrix}. \quad (5)$$

This transfer matrix can be made available in practice using a mixed nonlinear/linear analysis framework for power systems like, e.g., [18]. More precisely, the nonlinear system is linearized around a given operation point and, next, the frequency response from all the modes can be made available by numeric computation of the frequency response even for the large-scale systems. Bode plots of two entries of $H(s)$ for the case of the ENTSO-E system are given in Fig. 3. A control model can be obtained from $H(s)$ if each of its entries $H_{ij}(s)$ is written as a limited order development plus a correction. Indeed, $H_{ij}(s) = \sum_{k=1}^n \frac{r_k^{ij}}{s-p_k}$, where r_k^{ij} denotes the residue of the pole p_k of H_{ij} . Obviously, n , the total number of poles of H , is huge since it equals the order of the full simulation model (between 8000 and 20000 for the European system). However, for the control model, the concerned dynamics are defined within the frequency band of the modes in the set Λ . We propose as control model the following approximation of $H_{ij}(s)$, $i, j \in \{1, \dots, m\}$:

$$\tilde{H}_{ij}(s) = \frac{A(s)}{B(s)} + \frac{P(s)}{Q(s)}; \quad \frac{A(s)}{B(s)} = \sum_{k=1}^l \left[\frac{r_k^{ij}}{s - \lambda_k} + \frac{\bar{r}_k^{ij}}{s - \bar{\lambda}_k} \right] \quad (6)$$

where r_k^{ij} , \bar{r}_k^{ij} , $k = 1, \dots, l$ are known (by \bar{r}_k^{ij} we denote the complex conjugate of r_k^{ij}) and the polynomials $P(s)$ and $Q(s)$ are computed such that $\tilde{H}_{ij}(s)$ fits $H_{ij}(s)$ in the frequency working band mentioned above.

2.3. Test system

The techniques for the synthesis of the control model and the PSS loops investigated in this paper are tested and illustrated on a realistic large-scale representation of the interconnected European. More precisely, this is a representation of the European power system before the interconnection with zone 2 (Romania and Bulgaria) and Turkey. It consists of about 2000 buses, 2400 lines and 810 transformers. The generators of which power is greater than 100MW (about 400 machines) are represented by detailed dynamic models along with the detailed models of their regulations. The rest of the generation is considered as static injection at the load-flow stage. A winter peak load scenario is considered. The resulting linear model is described by about 8000 state variables. It is well-known that this system exhibits a low damped inter-area oscillation around 0.22 Hz in which the generators of the eastern part of the grid are oscillating against the generators of the western part [17]. This phenomenon is represented by the first two modes of the linearized full model of which dampings are given in the first line of Table 1.

They are studied in this paper along with the one in the third column of the same table which is of different nature; it is an inter-area mode of the Spanish system at a slightly higher frequency (0.9 Hz) than the first two ones. It is chosen here along with the slow ones (#1 and #2) in order to be in the situation which requires the "second level of coordination" mentioned in the Introduction. Thus, one has (6) with $l = 3$ and λ_k , $k = 1, \dots, 3$ given in Table 1.

2.4. Frequency identification of the parameters of the control model

The degrees of the polynomials P and Q in (3) are chosen such that \tilde{H}_{ij} is strictly proper:

$$Q(s) = s^v + q_{v-1}s^{v-1} + \dots + q_0, \quad P(s) = p_{v-1}s^{v-1} + \dots + p_0 \quad (7)$$

To obtain a control model of order $2l + v$, $2v$ parameters have to be identified as coefficients of P and Q . This is done using the Bode plots of the $H_{ij}(s)$ as in Fig. 3. They contain information in the wide frequency range of the full simulation model (*i.e.*, about 8000 poles). However, for the stabilization problem we want to solve here, only the frequency range $[\omega_\Lambda^- \ \omega_\Lambda^+]$ which covers the set of modes Λ is of interest. For the chosen test system, this range is defined around the two major resonance peaks in Fig. 3 which correspond to λ_1 and λ_3 in Table 1 (the frequency of λ_2 is in between), *i.e.*, $\omega_\Lambda^- = 0.15$ Hz, $\omega_\Lambda^+ = 2$ Hz.

An adequate control model should fit the Bode plots of the full simulation model in the frequency range $[\omega_\Lambda^- \ \omega_\Lambda^+]$.

The coefficients p_i , q_i in (7) of each transfer $\tilde{H}_{ij}(s)$ in (6) are thus computed via a frequency identification procedure based on a least squares objective function of the form

$$J_{ident} = \sum_{\omega_\Lambda^- \leq \omega_k \leq \omega_\Lambda^+} [\alpha_k (A_k - |\tilde{H}_{ij}(i\omega_k)|)^2 + \beta_k (\varphi_k - \arctg(\tilde{H}_{ij}(i\omega_k)))^2] \quad (8)$$

where A_k and φ_k are the values of the magnitude and respectively the phase of $H_{ij}(i\omega_k)$ and $i^2 = -1$. (A_k, ω_k) and (φ_k, ω_k) are points of the Bode plots of the transfer of the full simulation model and are thus input data for the frequency identification problem

$$\{p_i, q_i\}_{i \in \{0, \dots, v-1\}} = \operatorname{argmin}\{J_{ident}\}. \quad (9)$$

The weights α_k, β_k are used to manage the trade-off between magnitude and phase fitting and, eventually, to give priority to the fitting at specific frequencies.

A stability constraint on the roots of Q could be used in (9) to ensure a stable control model $\tilde{H}_{ij}(s)$.

This identification is repeated as a trial and error iterative procedure with increasing degrees for the polynomials P and Q above till an acceptable frequency response fitting is achieved.

Such a situation is shown in Fig. 3a for a transfer function of the diagonal of $H(s)$. The responses of the full model are in solid lines and the reduced model is obtained with $\deg(P) = 1$ and $\deg(Q) = 2$, i.e., for a control model of order 8. For the transfers of the extra diagonal entries of H the fitting is more difficult since interactions among different machines should be captured. Fig. 3b shows the result obtained with the same order ($v = 2$) for two Spanish machines ($i = \text{Almaraz}, j = \text{Cofrentes}$). The resulting numerical values are given in Table 2. They were obtained with equal weights ($\alpha_k = \beta_k = 1$ for all k) and using standard Matlab routines (fminsearch/lsqnonlin). If necessary, accuracy of the identification can be further increased by increasing v . However, the order 2 has been retained for the example treated in this paper since the tuning provided with this model was satisfactory. Indeed, the main objective here is to tune with the simplest control model.

3. Optimal tuning of PSSs

The control model (6) is used to simultaneously tune the PSSs of the machines in the set M for desired target values ζ_i^{ref} , $i = 1, \dots, l$ of the damping of the modes in Λ . To ensure a standard IEEE structure for the PSSs, like, e.g.,

$$\frac{V_s(s)}{\omega(s)} = K \frac{1 + T_1 s}{1 + T_2 s} \frac{1 + T_3 s}{1 + T_4 s} \frac{T_5 s}{1 + T_6 s}, \quad (10)$$

(see [11]) the problem is formulated as an optimization one which gives an optimal set of gains and time constants for each machine (K and T_i in (10)) in the set M .

3.1. The objective function

The objective function to be minimized should capture the dynamic performance specified, basically the damping of the oscillatory response of the system. In [19] and [13] a *modal objective function* is proposed:

$$J_{contr} = \sum_{k=1}^l [(a_k \Psi(\sigma_k, \omega_k) \sum_{i=1}^m \sum_{j=1}^m r_k^{ij} \bar{r}_k^{ij})]^{1/2} \quad (11)$$

$$\Psi(\sigma_k, \omega_k) = \frac{\sigma_k^2 + \omega_k^2}{2\sigma_k^3} \left(e^{\frac{2\sigma_k^3 T}{\sigma_k^2 + \omega_k^2}} - 1 \right)$$

where r_k^{ij} is the residue of the mode $\lambda_k = \sigma_k \pm j\omega_k$ in the transfer $H_{ij}(s)$, a_k a weighting function ($a_k = 1$ if λ_k is real and $a_k = 2$ if λ_k is complex) and $T > 0$ is the time horizon over which J_{contr} is evaluated.

Roughly speaking, (11) contains the integral of the surface under the modal response envelope through a given time horizon T . First, the computation of this function is not straightforward in practice and, next, minimizing J_{contr} given by (11) leads to a response with *maximum* damping which is not necessarily needed. Indeed, only the level ζ_i^{ref} , $i = 1, \dots, l$ of damping is required and not going below would allow one to settle a better trade-off robustness/performance (see, e.g., [20]). This led us to test a simpler and more direct index of performance:

$$J_{contr} = \sum_{i=1}^l (\zeta_i - \zeta_i^{ref})^2. \quad (12)$$

Relation (3) can be exploited to obtain in a simplified manner the influence of the adjustment of the gains of the PSSs on the modes in Λ . Moreover, to reduce the size of the problem, it is considered that $T_3 = T_1$ and $T_4 = T_2$ in (10). The optimal PSS parameters are thus:

$$\{K_i^*, T_1^*, T_2^*\} = \operatorname{argmin}\{J_{contr}\} \quad (13)$$

where J_{contr} is now given by (12). The above objective functions have been compared on the Single Machine Infinite Bus (SMIB) system in Fig. 5 of which parameters are given in Appendix 1. Without the use of a PSS, the inter-area mode of this system is $-0.0227 \pm j0.4951$, i.e., of damping $\zeta_0 = 4.58\%$. Problem (13) solved with (12) for $\zeta^{ref} = 10\%$ leads to $K = 46pu$, $T_1 = 2.17s$ and $T_2 = 2.24s$ which improve

in closed-loop the damping of the above inter-area mode to $\zeta = 10\%$. The same problem solved with (11) instead of (12) leads to $K = 49.01pu$, $T_1 = 4.01s$ and $T_1 = 4.01s$ which provide a damping of $\zeta = 0.1075$. In this latter case the gain is larger and the damping is (a little) higher than the target. This is normal because in this case the damping target is not directly taken into account into the optimization as with (12). The trade-off between the gain magnitude and the obtained damping can be managed by adding constraints to problem (13) as explained in the section below.

3.2. The constraints

Several types of constraints may be considered with (13) or (11). First, physical bound constraints

$$\begin{cases} T_{1_i} \geq 0 \\ T_{2_i} \geq 0 \\ K_i \geq 0 \end{cases}, i \in \{1, \dots, m\} \quad (14)$$

contain the physical bounds for the gains and the time constants of the PSSs. An additional upper bound $K_i \leq K_i^{max}$ can be added to (14) to ensure implementable solutions, *i.e.*, to avoid mathematical solutions with unrealistic high gain. Next, several nonlinear constraints are added. The main one consists in a stability condition of the resulting closed-loop ($H(s)$ feedback connected with $\Gamma(s)$ in Fig. 1. The eigenvalues of state matrix of the closed-loop should be in the left-half plane:

$$Max\{Re(\lambda_k^{cl})\} < 0, k \in \{1, \dots, 2l + v + 3m\}. \quad (15)$$

Notice that λ_k^{cl} are functions of K_i , T_{1_i} and T_{2_i} of the PSSs $\Gamma(s)_i$ of type (10). In [13] and [21], it was shown how constraints given by H^∞ -norm of adequate transfer functions may be used to ensure robustness.

3.3. Validation on the European power system

For the test system presented in Section 2.3, the Spanish machines Almaraz, Cofrentes and PGR were chosen to damp the modes selected in Table 1 since they have high participation in these modes and they are not already equipped with PSSs. The damping target is $\zeta^{ref} = 10\%$ for each of the three modes. This objective is interpreted as follows: mode #1 is poorly damped and ζ_1 should thus be increased, but

the damping actions should be chosen in order to not degrade the damping of the other two modes, one directly concerned by the east-west oscillation and the other one local to the Spanish system.

3.3.1. Linear validation

The results obtained minimizing (13) (first position in Table 3) are compared with the ones provided by the tuning proposed in [3] where only a static control model is used (second position in the same Table 3). First, the gains obtained with the procedure presented above are lower than the ones in [3] and thus the robustness is improved in general. This difference can also be noticed in the Bode plots of the open-loop transfer functions of the control system, i.e., of $\Gamma_i(s)H_{ii}(s)$, given in Fig. 2 for $i = Almaraz$. The damping factors obtained when the optimal parameters are used for PSSs are given in the second line of Table 1. Also, notice that only two machines (Almaraz and Cofrentes) are needed to reach the damping objectives with the tuning procedure presented here since the gain obtained for PGR is $K^* = 0$ as shown in Table 3. Notice that for this example no robustness constraints have been taken into account. The optimization problem (13) has been solved with standard Matlab routines (fmincon).

3.3.2. Full nonlinear validation

It is now shown that the damping level achieved in the preceding section using linear models is still valid in nonlinear simulation. For the latter validation, the system is simulated in detail using the Eurostag software for transient stability analysis [14]. Fig. 4 gives the speed responses of machines Almaraz to a short-circuit of 200ms at the grid connection point of the same machine. It can be seen that the damping of the response is improved (the more damped curve corresponds to the situation when the 2 PSSs described in the first entries of Table 3 are used), while the less damped response is obtained on the initial situation when no PSSs are used on the machines in the set M).

Remark

Notice that, as shown in Table 1, that damping target $\zeta^{ref} = 10\%$ is achieved for mode #3 and (almost for) mode #2 but not for mode #1 although the damping of the latter mode has been significantly improved. This is normal since it is the result of a constrained optimization. From the physical point of view, this means that the damping means are not sufficient. To further improve the damping in these

situations, the class M of machines on which PSS are installed/tuned should be enlarged.

4. Coordinated tuning of PSSs and governors

In this section it is shown in which cases interactions between the PSS and governor dynamics may occur and how they can be overcome.

4.1. Interactions PSSs/governors

Consider first the simplest situation of the SMIB system in Fig. 5. This system has an inter-area mode which frequency depends (mainly) on the inertia H of the generator and the reactance X of the line. The latter parameters (given in Appendix 1 along with all the data of the test system) are chosen such that the frequency of this mode is $f = 0.07\text{Hz}$. This simple example reproduces a type of inter-area mode which exists on a large-scale power system with weak interconnections as the one treated in Section 5.3.

When a standard AVR is used, this mode is poorly damped ($\zeta = 0.93\%$) as shown by the solid line response in Fig. 6a to a 100ms short-circuit applied at the generator bus.

If a PSS loop is added, the oscillations are damped as shown by the response in dotted line in the same figure. The PSS structure (10) with $T_1 = T_3$ and $T_2 = T_4$ was used and its parameters have been tuned for the target $\zeta^* = 7.5\%$ with the classical technique based on the residues recalled in Section 2.1. This led to

$$K_{PSS} = 49.7\text{pu}, T_{1PSS} = 2.3\text{s}, T_{2PSS} = 2.13\text{s}. \quad (16)$$

The latter two simulations have been carried out only with voltage regulations for the machine, i.e., its mechanical torque has been considered constant. This is the usual way of tuning the PSS since the voltage and mechanical dynamics are sufficiently decoupled (in frequency) to be considered independent. In other words, the adjustment of the voltage regulators have no, or little influence, on the turbine regulation and vice versa. As a consequence, the two classes of regulators are synthesized independently and, afterwards, used together on the machine. This is no longer valid in the situation considered in this paper. Indeed, if the frequency of the modes to be damped by the PSS is too low, the voltage correction actions may

act also on the turbine and vice versa. Consider the structure in Fig. 7 which corresponds to a standard governor if the lead-lag bloc in dotted line is not used (i.e., $T_{1GOV} = T_{2GOV} = 0$). In this case, a phase lag action is induced by the PI bloc in Fig. 7. If the PSS is tuned for a frequency close to the governors dynamics and if it should provide a phase lead (as it is the case for the parameters (16)), this action is thus diminished by the PI bloc of the governor and the PSS is thus less efficient when used in conjunction with the governor. This is the case of the example treated here. If the governor presented above with $R = 20pu$, $K_P = 0.5pu$, $T_I = 10s$ is used in conjunction with the PSS tuned before, the damping target is no longer achieved as shown by the response in dotted line in Fig. 6a.

4.2. Mixed control synthesis

To overcome the problem formulated in the section above, the structure of the governor has been enriched with the lead-lag filter in dashed line in Fig. 7. This allows one to shape the frequency profile of the governor without modifying the parameters obtained for the initial design and which ensure the turbine performances, i.e., the droop R , the gain K_P and the time constant T_I of the PI bloc. The tuning of the parameters T_{1GOV} and T_{2GOV} of this new lead-lag filter is done simultaneously and in a coordinated way with the tuning of the parameters of the PSS. They are the result of an constrained optimization of the costs function (12) as in Sections 3.1 and 3.2. Notice, that in this process, the parameters R , K_P and T_I are considered as constants. For the SMIB example presented in Section 4.1, the target of this optimization is $\zeta^* = 10\%$ and it is reached with $K_{PSS} = 48.9pu$, $T_{1PSS} = 0.48s$, $T_{2PSS} = 0.62s$, $T_{1GOV} = 1.17s$ and $T_{2GOV} = 0.26s$. This can also be checked with the response of the nonlinear simulation in solid line in Fig. 6b obtained with the latter parameters.

The same situation is reproduced on the 4-machines test system in Fig. 8 of which parameters are given in Appendix 1. Indeed, the lines NHVC1-NHVA1, NHVC1-NHVD1 and NHVC2-NHVB1 are longer than the other branches of the grid and, as a consequence, the inter-area mode related to the swing of generator GENC against the three machines in the south of the system is of low frequency (0.1Hz) and poorly damped. This mode can be observed in solid line in Fig. 9a which shows the responses to a short-circuit at bus NHVCEQ. This mode is damped when a standard PSS is added to machine GENC (dotted-line response in Fig. 9a) but this improvement is lost when a standard governor is also used for the same machine. In the latter case, the system is unstable (dashed-line response in Fig. 9a). As in the SMIB case, this

problem is overcome with the coordinated synthesis of the PSS-governor for which satisfactory responses are obtained as shown in Fig. 9b (solid line).

5. General multi-level tuning procedure

The results of sections 2, 3 and 4.2 are now aggregated into a general control procedure in order to satisfy the three levels of coordination described in the Introduction.

5.1. General control model

The control model introduced in Section 2 is extended in order to take into account also the dynamics of the turbines of the m generators selected for the control. It consists of the transfer matrix $H(s)$ in Fig. 10 defined by

$$\begin{bmatrix} P \\ \omega \end{bmatrix} = H(s) \begin{bmatrix} P_m \\ V \end{bmatrix} \quad (17)$$

where $P = [P_1 \dots P_m]^T$ is the vector which contains the electrical powers of the involved machines, $\omega = [\omega_1 \dots \omega_m]^T$ the vector of the rotor speeds, $P_m = [P_{m_1} \dots P_{m_m}]^T$ the vector of the mechanical powers and $V = V_{ref} - V_S$ with $V_{ref} = [V_{ref_1} \dots V_{ref_m}]^T$ the vector of references of voltage control loops, $V_S = [V_{S_1} \dots V_{S_m}]^T$ the vector of the PSS outputs, $\Gamma(s) = \text{diag}\{\Gamma_1(s), \dots, \Gamma_m(s)\}$, $\bar{\Gamma}(s) = \text{diag}\{\bar{\Gamma}_1(s), \dots, \bar{\Gamma}_m(s)\}$ where $\Gamma_i(s)$ is the transfer function of the PSS of machine i , $\bar{\Gamma}_i(s)$ is the transfer function of the governor of machine i and $i \in \{1, \dots, m\}$.

Using the methodology given in Section 2, a reduced order representation is constructed for the transfer matrix $H(s)$ defined above in the range of frequency of the modes to be damped (in the set Λ).

5.2. Tuning procedure

The control model above is used to tune the parameters of the PSSs Γ_i , $i = 1, \dots, m$ and of the lead-lag filters of the governors $\bar{\Gamma}_i$, $i = 1, \dots, m$. The same procedure based on the constraint optimization technique given in Section 3 can be used. The main

control objective is the damping of the modes directly taken into account in the cost function (12). Stability and robustness specifications can be taken into account by adding supplementary constraints to the optimization problem

$$\{K_i^*, T_{1,i}^*, T_{2,i}^*, T_{1GOV_i}^*, T_{2GOV_i}^*\} = \operatorname{argmin}\{J_{contr}\} \quad (18)$$

as shown in Section 3, [13] and [21].

5.3. Large-scale test

The general methodology summarized in the preceding section has been applied to a large-scale power system. A benchmark has been constructed from the ENTSO-E model presented in Section 2.3 as follows: the dynamic model has been triplicated and the three samples have been interconnected as shown in Fig. 11. The resulting benchmark reproduces in an exploitable manner the interaction phenomena described in the Introduction. More precisely:

- the resulting power system model has a realistic large-scale. It consists of about 1200 generators which is the actual size of the European interconnected power system (which includes Romania, Bulgaria and Turkey zones).
- the series interconnection in Fig. 11 generates a low-frequency inter-area mode. The most involved machines are among the nuclear plants of the French zone. The shape of the oscillation is zone ENTSO-E 2 against ENTSO-E 1 and 3 in Fig. 11 and the frequency of the mode is $0.09Hz$. Indeed, Fig. 12 provides in dashed and dashed-dotted lines the speed responses of machines BUGEY of zones ENTSO-E 2 and 3 to a 150ms short-circuit at the connection bus of machine BUGEY of zone ENTSO-E 2. It can be noticed the phase opposition of the two oscillatory responses as well as a common period which correspond to the frequency of the mode. If the specific four-loops voltage regulators (see, e.g., [22] and related references) which control the French nuclear plants is replaced by a standard IEEE AVR (type IEEE X4 - Type 4 excitation system) [11] without PSS for the three most participant machines in the oscillation (namely BUGEY, GRAVELINE and PALUEL in zone ENTSO-E 1), the damping of the aforementioned mode drops to $\zeta = 3.48\%$ (see again the two responses aforementioned). The context is thus similar to the one of [7] in which a very spread and poorly damped inter-area mode has been put into evidence at $0.07Hz$.

- in opposition to study [7], this benchmark is exclusively constructed with European data.

When the target damping of the inter-area mode mentioned above is fixed at $\zeta^{ref} = 10\%$, the control synthesis methodology given in Section 5.2 leads to the optimal parameters given in Table 4 for the three French machines chosen for the control in zone ENTSO-E 1. The obtained parameters have been implemented in the structures given by (10) and Fig. 7 on the selected machines in the nonlinear model of the interconnected benchmark in Fig. 11. The speed response of machine BUGEY of zone ENTSO-E 2 given in solid line in Fig. 12 shows that the tuned regulators are efficient, i.e., the target value of 10% of the damping of the inter-area mode is reached.

Remark

Notice that in the methodology of the mixed-control proposed in Sections 4.2 and 5.2 the governor structure is only modified by adding a lead-lag filter (Fig. 7) which is tuned on the frequency of the inter-area modes which have to be damped. It acts thus only when the latter modes are excited and its impact in these situations on the mechanical torque is limited as shown in Fig. 13a. This figure shows the response of the mechanical torque of one of the machines used for the synthesis presented for the large-scale test to the short-circuit at its grid connection point which excites the target low-frequency (0.09Hz) inter-area mode. Also, the initial function of the governor is not deteriorated by the added lead-lag filter as shown by the response in Fig. 13b to a 3% step increase of the power reference of the same machine.

6. Conclusions

This paper shows how several levels of coordination can be simultaneously achieved for the synthesis of PSSs. These coordinations, especially the one between the tuning of the PSSs and of the governors of the chosen generators, opens the way to stabilize very large interconnected power systems in which the frequencies of the slowest inter-area modes come into the turbine frequency range. The size and the structure of the actual European interconnected power system are close to the conditions mentioned above. The next potential extensions of this system [23], [7] might cause such interactions and the methodology presented here is a way to overcome these difficulties.

The principles of coordination presented here can be applied to other types of PSSs like, e.g., the multi-band PSS [11], [4] or to coordinate the damping actions of the

generators with the ones of other grid devices as, for example, some FACTS (see [24] and related references).

The key point of the proposed methodology is the use of an efficient control model for the synthesis of the control laws which allows, in particular, to deal with the large-scale systems. This model is built to take into account the interactions of the main dynamics of the system.

The parameters of the regulators are computed via a constraint optimization in order to keep standard structures for the PSSs and governors. First, the constraints of this problem can be adapted in order to ensure different aspects of performances and robustness (especially by taken into account several operating points of the system) for the resulting closed-loop as shown, for example, in [25] and related references. Next, algorithms with better performances may be used to solve the optimization problem (18). Indeed, the optimization methodologies have been the subject of ongoing enhancements over the years. A review of the most used in power systems is given in [26]. Finally, the optimization itself can be replaced by a synthesis technique with better performances if new structures (like, e.g., state-space forms) are allowed for the regulators instead of the actual standard ones. From this point of view, the methodology presented here is an open framework.

Acknowledgment

The authors would like to thank Dr. B. Mallem for preliminary investigations on the topic of governors control at the end of his Ph.D stay at RTE.

Appendix 1: Data of the test systems

SMIB test system (Fig. 5):

generator parameters (no load pu):

stator resistance 0.005pu, stator leakage 0.219pu, direct reactance 2.57pu, direct transient reactance 0.422pu, direct sub-transient reactance 0.3pu, direct transient time constant 7.695s, direct sub-transient time constant 0.061s, quadrature reactance 2.57pu, quadrature transient reactance 0.662pu, quadrature sub-transient reactance 0.301pu, quadrature transient time constant 0.643s, quadrature sub-transient time constant 0.095s, inertia 50MWs/MVA

block transformer: 24kV/400kV, rate 1.1pu, R=0.005pu, X=0.005pu (base 24kV)

regulators:

AVR: $EFD = K \frac{K_e}{1+sT_e} (V_{ref} - V_t)$, $K=40pu$, $T_e=0.1s$, $K_e=1pu$;

GOVERNOR: constant mechanical power

the line: $R=0pu$, $X=0.7pu$ ($S_{base}=100MVA$ and $V_{base}=400kV$)

load-flow: $P=100MW$, $Q=35MVar$, $V=24kV$, $V_{inf}=400kV$

Intermediate-scale test system (Fig. 8):

common generators' parameters: the same as for SMIB

generators' inertias [MW s/MVA]: GENA1 10, GENB1 5, GENB2 5, GENC 10

block transformers: 24kV/380kV, rate=1.1pu, $X=0.00769pu$ for GENA1, $X=0.02251pu$ for GENB1, $X=0.09pu$ for GENB2, $X=0.00769pu$ for GENC (base 24kV)

regulators:

AVR of each machine: the same as for SMIB with $K_e=1pu$; $K=40pu$; $T_e=0.1s$ for GENA1 and GENB1 and $K=30pu$; $T_e=1s$ for GENB2 and GENC

GOVERNOR for GENA1, GENB1, GENB2: $T_m = \frac{1}{1+0.1s} \frac{1}{1+0.5s} \frac{1+3s}{1+10s} (1 - \omega)$

standard PSS of machine GENC: $K = 1.07pu$, $T_1 = 3.11s$, $T_2 = 0.73s$

optimal PSS of machine GENC: $K = 4.32pu$, $T_1 = 3.09s$, $T_2 = 1.67s$

optimal GOVERNOR of machine GENC: $T_1 = 2.39s$, $T_2 = 2.52s$

generation and load:

NGENA1: $P=900MW$, $Q=300MVAR$, $V=24kV$

NGENB1: $P=400MW$, $Q=190MVAR$, $V=24kV$

NGENB2: $P=900MW$, $Q=300MVAR$, $V=24kV$

NGENC: $P=2504MW$, $Q=1500MVAR$, $V=24kV$

NHVA1: $P=-1000MW$, $Q=-100MVAR$ NHVB1: $P=-1000MW$, $Q=-300MVAR$

NHVC1: $P=-500MW$, $Q=-100MVAR$ NHVC2: $P=-600MW$, $Q=-200MVAR$

NHVCEQ: $P=-700MW$, $Q=-150MVAR$

line reactances [pu] ($S_{base}=100MVA$ and $V_{base}=380kV$):

NHVC1-NHVA1: 0.490 NHVC2-NHVB1: 0.5

NHVD1-NHVC1: 0.500 NHVC1-NHVC2: 0.011

NHVD1-NHVB1: 0.011 NHVCEQ-NHVC1 and 2: 0.22

NHVA3-NHVD1: 0.011 NHVA3-NHVA1: 0.02

References

- [1] G. Rogers, *Power System Oscillations*, Norwell, MA: Kluwer, 2000.

- [2] R. Gupta, B. Bandyopadhyay and A.M. Kulkarni, "Design of Decentralized Power System Stabilizers for Multimachine Power System using Model Reduction and Fast Output Sampling Techniques", *Proc. Asian Control Conference*, 2004.
- [3] L. Rouco, "Coordinated Design of Multiple Controllers for Damping Power System Oscillations", *International Journal of Electrical Power and Energy Systems*, Vol.23, No.7, pp. 517-530, October 2001.
- [4] R. Grondin, I. Kamwa, L. Soulieres, J. Potvin and R. Champagne, "An Approach to PSS Design for Transient Stability Improvement through Supplementary Damping of the Common Low-Frequency", *IEEE Trans. on Power Systems*, Vol. 8, No. 3, pp. 954-962, August 1993.
- [5] I. Kamwa, G. Trudel, L. Gerin-Lajoie, "Low-Order Black-Box Models for Control System Design in Large Power Systems", *IEEE Trans. on Power Systems*, Vol. 11, No. 1, pp. 303-311, February 1996.
- [6] I. Kamwa, D. Lefebvre and L. Loud, "Small Signal Analysis of Hydro-Turbine Governors in Large Interconnected Power Plants", *Proc. of IEEE Power Engineering Society Winter Meeting*, pp. 1178-1183, 2002.
- [7] M. Luther, I. Biernaka and D. Preotescu, "Feasibility Aspects of a Synchronous Coupling of the IPS/UPS with the UCTE", *CIGRE Session*, Paper C1-204, Paris, 2010.
- [8] F.R. Schleif, G.E. Martin and R.R. Angell, "Damping of System Oscillations with a Hydrogenerating Unit", *IEEE Trans. on Power Apparatus and Systems*, vol. PAS-86, No. 4, pp. 438-442, April 1967.
- [9] L. Kiss and J. Zerényi, "Realization of a "Band-Stop" Device to Damp Inter-Area Oscillations with Intervention into the Turbine Governor", *Proc. of PowerTech Conference*, Bucharest-Romania, 2009.
- [10] F.A. Okou, O. Akhrif and L.-A. Dessaint, "Decentralized multivariable voltage and speed regulator for large-scale power systems with guarantee of stability and transient performance", *International Journal of Control*, Vol.78, No.17, pp. 1343-1358, November 2005.
- [11] IEEE Power Engineering Society, "IEEE Recommended Practice for Excitation System Models for Power System Stability Studies", *IEEE Std 421.52005 (Revision of IEEE Std 421.5-1992)*, IEEE April 2006.

- [12] I. Kamwa, G. Trudel and D. Lefebvre, "Optimization-Based Tuning and Coordination of Flexible Damping Controllers for Bulk Power Systems", Proc. of *IEEE International Conference on Control Applications*, August 1999.
- [13] I. Kamwa, G. Trudel and L.Gérin-Lajoie, "Robust Design and Coordination of Multiple Damping Controllers Using Nonlinear Constraints Optimization", Proc. of *PICA*, 1999.
- [14] B. Meyer and M. Stubbe, "Eurostag, a Single Tool for Power System Simulation", Proc. of *IEEE Conf. on Transmission and Distribution*, March 1992.
- [15] G.N. Taranto, A.L.B. do Bomfim, D.M. Falcao, N. Martins, S. Gomes, P.E. Quintao, "Combined use of Analytic and Genetic Algorithms for Robust Coordinated Tuning of Power System Damping Controllers", Proc. of *Bulk Power System Dynamics and Control IV-Restructuring Conference*, August 24-28, Santorini (Greece), 1998.
- [16] L. Rouco, I.J. Pérez-Arriaga, R. Criado and J. Soto, "A computer Package for Analysis of Small Signal Stability in Large Electric Power Systems", Proc. of the *11th Power Systems Computations Conference*, pp. 1141-1148, Avignon (France), August 1993.
- [17] H. Breulmann et al., "Analysis and Damping of Inter-area Oscillations in the UCTE-CENTREL Power-System", *CIGRE Session*, Paper 38-113, Paris, 2000.
- [18] B. Marinescu and L. Rouco, "A Unified Framework for Nonlinear Dynamic Simulation and Modal Analysis for Control of Large-Scale Power Systems", Proc. of *Power Systems Computations Conference*, Liège-Belgium, August 2005.
- [19] J.B. Simo, I. Kamwa, G. Trudel and S.-A. Tahan, "Validation of a new modal performance measure for flexible controllers design", *IEEE Trans. on Power Systems*, vol. 11, no. 2, pp. 819-826, May 1996.
- [20] S. Skogestad and I. Postlethwaite, *Multivariable Feedback Control*, John Wiley and Sons Ltd., Chichester-England, 1996.
- [21] B. Marinescu, B. Mallem, H. Bourlès and L. Rouco, "Robust Coordinated tuning of Parameters of Standard Power Systems Stabilizers for Local and Global Grid Objectives", Proc. of *Power Tech Conference*, June 28th-July 2nd, Bucharest, Romania, 2009.

- [22] R. Bénéjean, P. Blanchet, J. P. Meyer and P. Hugoud “A New Voltage Regulator for Large French Alternators”, Proc. of *CIGRE Conf.*, vol. 32-13, 1982.
- [23] CE-ENTSO-E, ”Feasibility Study on the Interconnection Variants for the Integration of the Baltic States to the EU Internal Electricity Market”, 2010-2013, http://www.litgrid.eu/go.php/eng/Strategic_projects/352/2/514.
- [24] L-J. Cai and I. Erlich, “Simultaneous Coordinated Tuning of PSS and FACTS Damping Controllers in Large Power Systems”, *IEEE Trans. on Power Systems*, Vol. 20, No. 1, pp. 294-300, February 2005.
- [25] R.A. Jabr, B.C. Pal and N. Martins, “A Sequential Conic Programming Approach for the Coordinated and Robust Design of Power System Stabilizers”, *IEEE Trans. on Power Systems*, Vol. 25, No. 3, pp. 1627-1637, August 2010.
- [26] M. Eslami, H. Shareef and A. Mohamed, “Power System Stabilizer Design Based on Optimization Techniques”, Proc. *Modeling, Simulation and Applied Optimization (ICMSAO)*, 2011.

Table .1: Damping ζ [%] of the modes in Λ

	mode #1 0.23Hz	mode #2 0.24Hz	mode #3 0.91Hz
without PSSs	3.87	11.7	6.25
with PSSs	8.43	9.97	11.53

Table .2: Coefficients of the control model used in Fig. 3a

	s^6	s^5	s^4	s^3	s^2	s^1	s^0
P(s)						0.001	-0.11
Q(s)					1	1.55	44.20
A(s)		-0.001	-0.01	-0.10	-0.30	-0.33	-0.52
B(s)	1	1.23	38.59	22.53	169.97	46.80	193.85

Table .3: Comparison of the stabilizer parameters achieved with coordinated tuning and with robust coordinated tuning

	$K^*[pu]$	$T_1^* = T_3^*[s]$	$T_2^* = T_4^*[s]$
Almaraz	0.59 / 2.43	0.22 / 0.21	0.05 / 0.02
Cofrentes	4.81 / 5.74	0.59 / 0.58	0.15 / 0.05
PGR	0 / 0.54	0.71 / 0.61	0.15 / 0.06

Table .4: Parameters tuned for PSSs and governors of the large-scale test system

	BUGEY	GRAVELINE	PALUEL
$K_{PSS}[pu]$	28.5	27.6	28.5
$T_{1PSS}[s]$	2.1	2.6	2.1
$T_{2PSS}[s]$	2.8	2.4	2.7
$T_{1GOV}[s]$	2.1	2.1	2.1
$T_{2GOV}[s]$	2.8	2.8	2.8

Table .5: Participations and right eigenvectors' phase for the 0.07Hz mode of the large-scale system

Zone ENTSO-2			Zones ENTSO-1 and 3		
Machine	Participation [%]	Phase [°]	Machine	Participation [%]	Phase [°]
2_BUGEYSF1	70.9	1.2	3_BUGEYSF1	20.6	-175.7
2_GRAVSF1	88.2	1.0	1_PENLYSF1	29	-165.1
2_PALUESF1	100	-0.4	1_PALUESF1	32.1	174.9

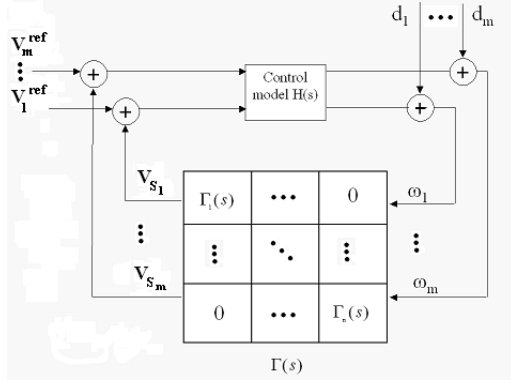


Figure .1: Control model

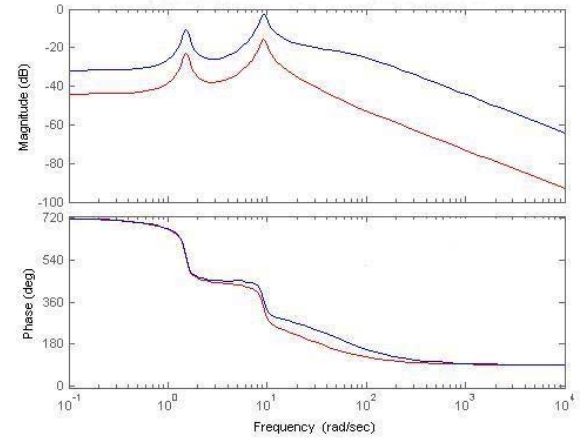
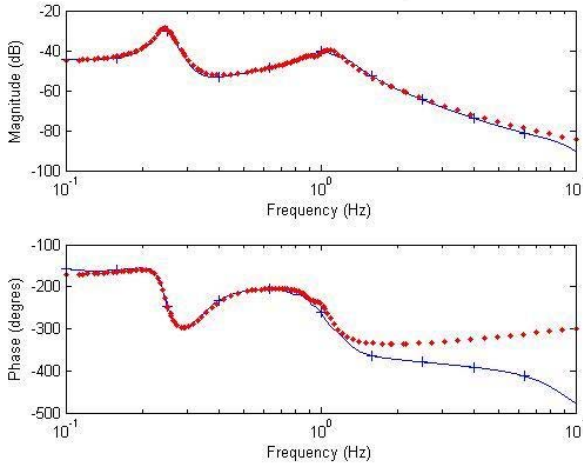
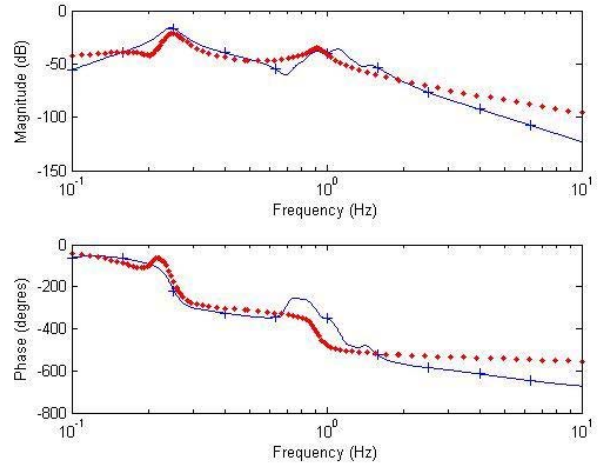


Figure .2: Bode plots of $\Gamma_i(s)H_{ii}(s)$, $i=Almaraz$: the coordinated control (blue '+' plot) and the robust coordinated control (red '.' plot)



(a) $H(s)_{ii}$, $i = PGR$



(b) $H(s)_{ij}$, $i = Almaraz$, $j = Cofrente$

Figure .3: Bode plots: the full model (blue '+' plot) and the control model (red '.' plot)

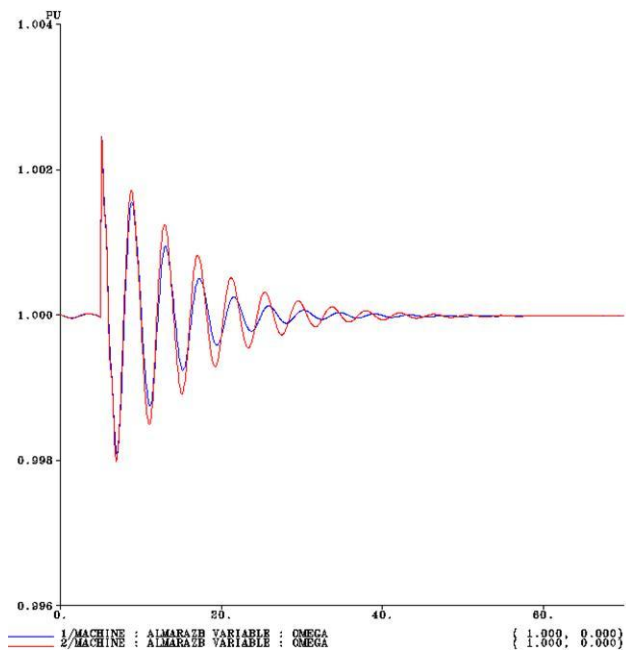
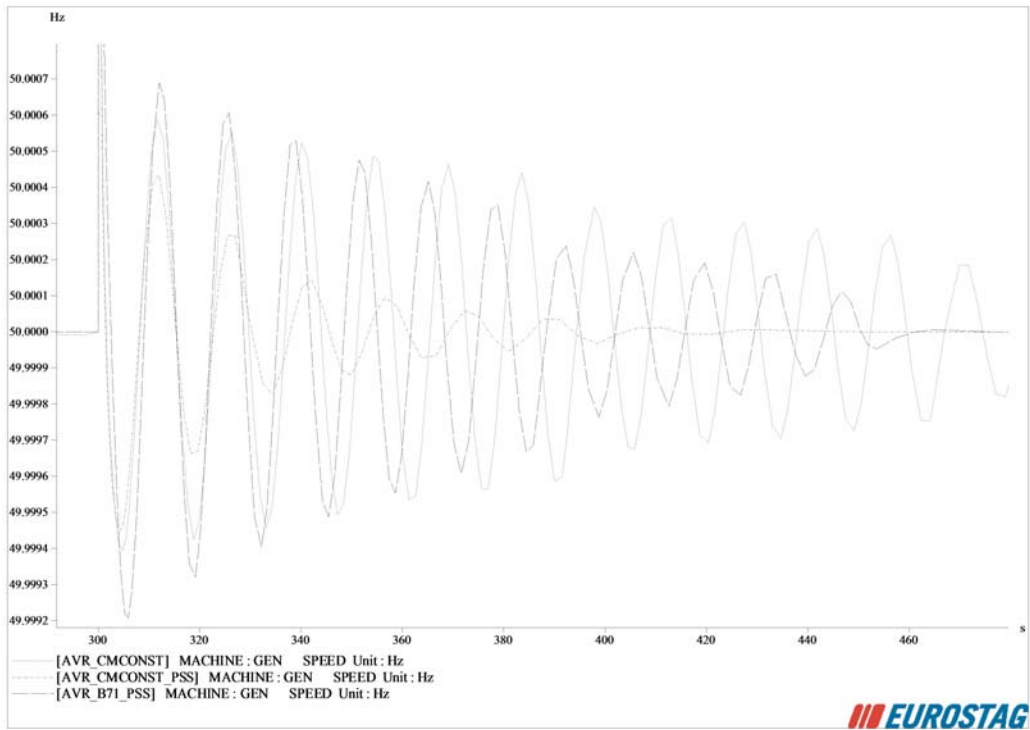


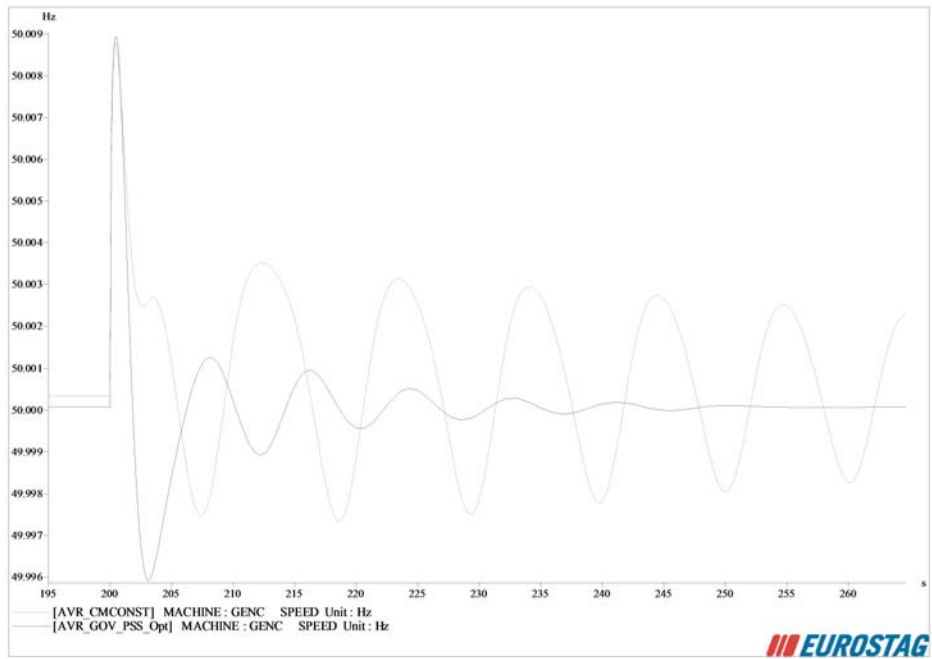
Figure .4: Nonlinear validation of the coordinated PSS tuning



Figure .5: SMIB test system: generator connected to an infinite bus



(a)



(b)

Figure .6: Short-circuit responses of the SMIB test system

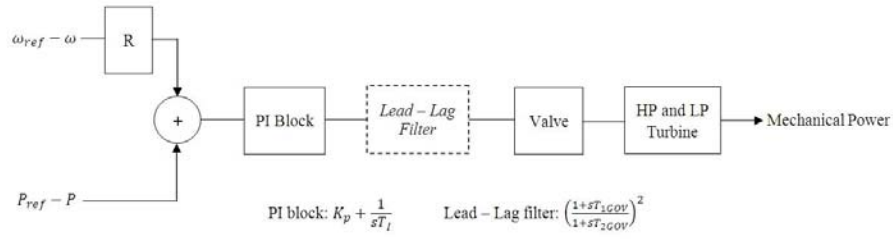


Figure .7: Structure of the improved governor

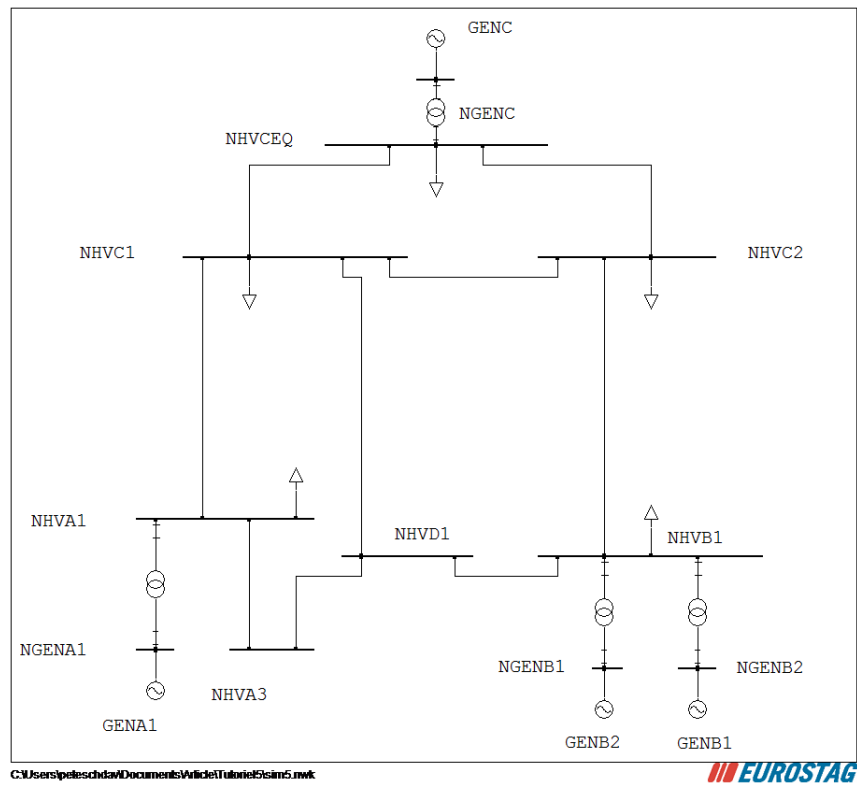
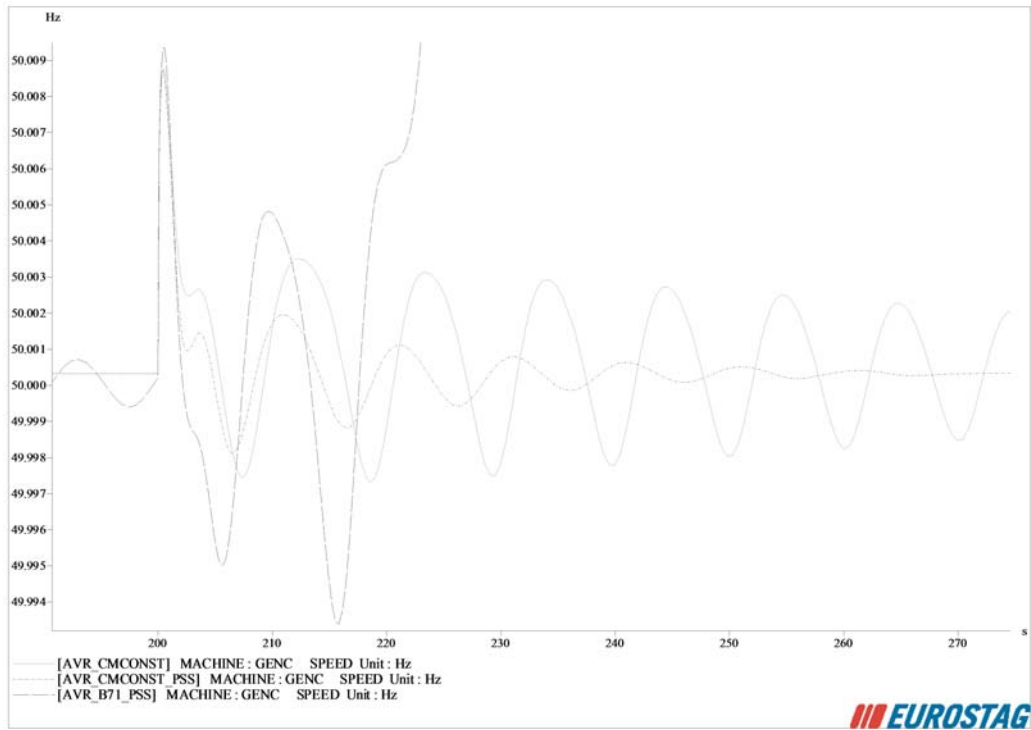
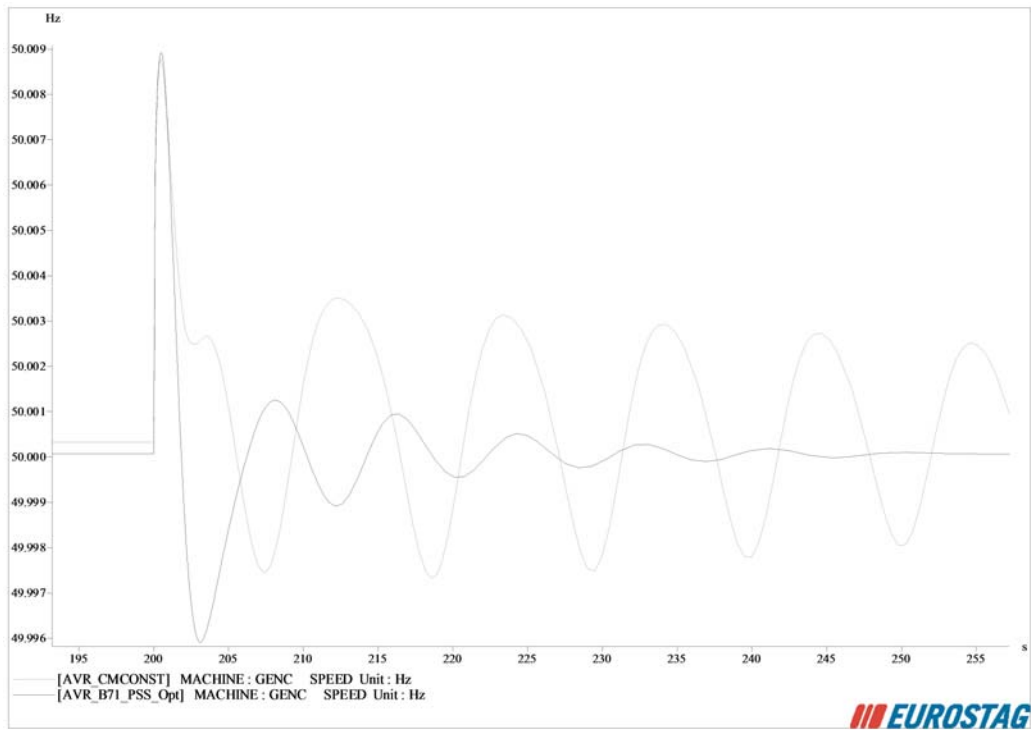


Figure .8: Medium-scale test system



(a)



(b) 27

Figure .9: Short-circuit responses of the medium-scale test system

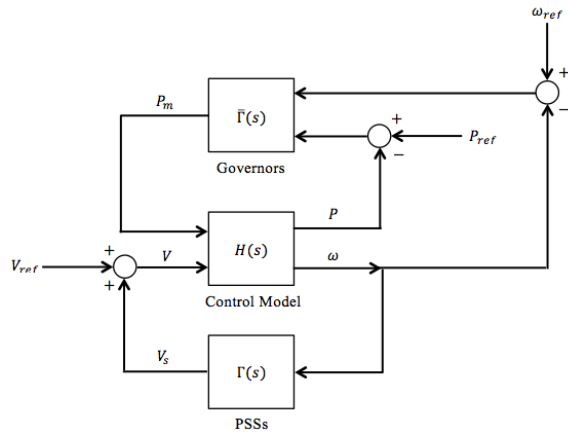


Figure .10: General control model

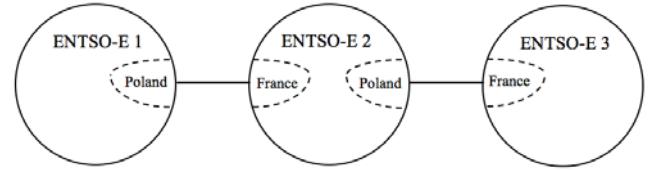


Figure .11: Large-scale test system

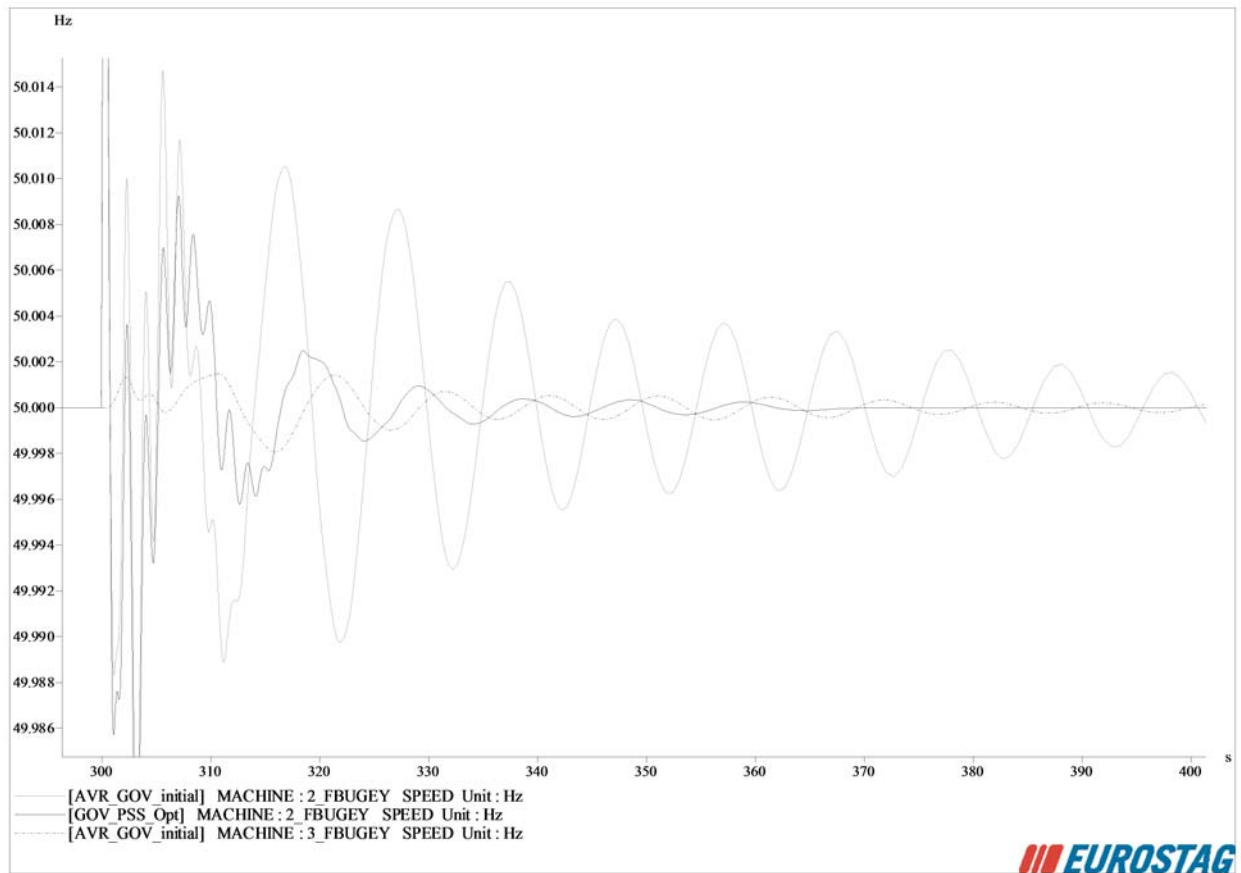
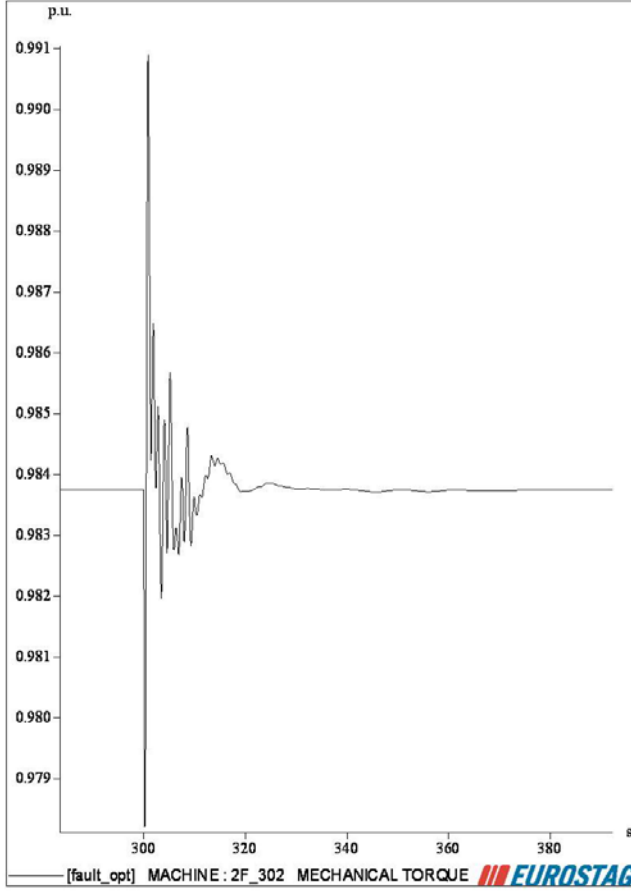
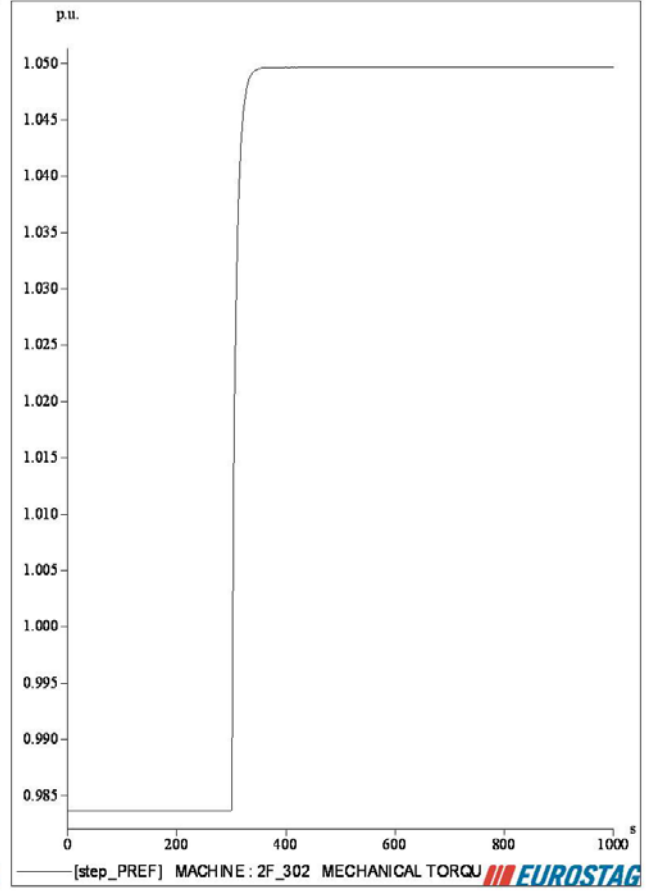


Figure .12: Short-circuit responses of the large-scale test system



(a) Short-circuit response



(b) Power step response

Figure .13: Responses of the mechanical torque